Environ Sci Pollut Res (2016) 23:24277–24288
DOI 10.1007/s11356-016-7691-0

RESEARCH ARTICLE

Sublethal concentrations of silver nanoparticles affect the mechanical stability of biofilms

Alexandra Y. Grün[1] · **Jutta Meier**[1] · **George Metreveli**[2] · **Gabriele E. Schaumann**[2] · **Werner Manz**[1]

Received: 11 April 2016 / Accepted: 12 September 2016 / Published online: 20 September 2016

Abstract Bacterial biofilms are most likely confronted with silver nanoparticles (Ag NPs) as a pollutant stressor in aquatic systems. In this study, biofilms of *Aquabacterium citratiphilum* were exposed for 20 h to 30 and 70 nm citrate stabilized Ag NPs in low-dose concentrations ranging from 600 to 2400 μg l^{-1}, and the Ag NP-mediated effects on descriptive, structural, and functional biofilm characteristics, including viability, protein content, architecture, and mechanical stability, were investigated. Viability, based on the bacterial cell membrane integrity of *A. citratiphilum*, as determined by epifluorescence microscopy, remained unaffected after Ag NP exposure. Moreover, in contrast to information in the current literature, protein contents of cells and extracellular polymeric substances (EPS) and biofilm architecture, including dry mass, thickness, and density, were not significantly impacted by exposure to Ag NPs. However, the biofilms themselves served as effective sinks for Ag NPs, exhibiting enrichment factors from 5 to 8. Biofilms showed a greater capacity to accumulate 30 nm sized Ag NPs than 70 nm Ag NPs. Furthermore, Ag NPs significantly threatened the mechanical stability of biofilms, as determined by a newly developed assay. For 30 nm Ag NPs, the mechanical stability of biofilms decreased as the Ag NP concentrations applied to them increased. In contrast, 70 nm Ag NPs produced a similar decrease in mechanical stability for each applied concentration. Overall, this finding demonstrates that exposure to Ag NPs triggers remarkable changes in biofilm adhesion and/or cohesiveness. Because of biofilm-mediated ecological services, this response raises environmental concerns regarding Ag NP release into freshwater systems, even in sublethal concentrations.

Keywords *Aquabacterium citratiphilum* · *monospecies* biofilm · Silver nanoparticles · Toxicity · Mechanical stability · Nanoparticle enrichment

Responsible editor: Thomas D. Bucheli

Electronic supplementary material The online version of this article (doi:10.1007/s11356-016-7691-0) contains supplementary material, which is available to authorized users.

✉ Alexandra Y. Grün
alexg@uni-koblenz.de

[1] Institute for Integrated Natural Sciences, University of Koblenz-Landau, Universitätsstr. 1, 56070 Koblenz, Germany

[2] Institute for Environmental Sciences, Group of Environmental and Soil Chemistry, University of Koblenz-Landau, Fortstr. 7, 76829 Landau, Germany

Introduction

Nanoparticles are typically specified as particles ranging from 1 to 100 nm in size (Lemire et al. 2013). In the case of silver nanoparticles (Ag NPs), their highly advertised antimicrobial properties have led to broad applications in consumer products (e.g., textiles, food packaging, surface treatment of medical devices, and household cleaning appliances). Today, Ag NPs hold a market share of 30 % of all currently registered nano-products (Reidy et al. 2013). Due to the large scale of use, increasing releases of Ag NPs into aquatic and terrestrial environments will result. Ag NPs will enter the aquatic environment mainly via sewage systems. Because sulfidization processes in sewage systems can be incomplete in wastewater treatment plants, Ag NPs are expected to be discharged into rivers at least partly in the metallic form (Kaegi et al. 2013). For natural aquatic systems, predicted environmental concentrations of Ag NPs range from 10 pg l^{-1} to 1 μg l^{-1} in the water

column and from 4 μg kg^{-1} to 14 mg kg^{-1} in sediments (Blaser et al. 2008; Gottschalk et al. 2013), but because these predicted concentrations are based on general assumptions without considering local conditions, actual accumulations will likely be highly variable. Furthermore, flood events may lead to a short-term release of Ag NPs into the water column resulting from sediment resuspension, as has been shown for a wide range of chemical compounds (Wölz et al. 2009). Within the riverine systems, Ag NPs are supposed to affect microbial biofilms (Kroll et al. 2015). Most microorganisms live in biofilms, i.e., embedded in a self-produced complex adhesive organic matrix located on almost every kind of native and man-made interface in aqueous systems. The biofilm matrix is formed of a hydrogel consisting mainly of water (97–99 %) (Christensen and Characklis 1990) and extracellular polymeric substances (EPS). In addition to extracellular DNA and polysaccharides, the bacterial EPS consist of considerable amounts of proteins (Flemming and Wingender 2010). These proteins are involved in controlling several characteristics of the biofilms, including structural integrity (Chaw et al. 2005), architecture, sorption of organic substances, and inorganic ions (Flemming and Wingender 2010) as well as mechanical stability (Mayer et al. 1999). The mechanical stability of the biofilms, which is characterized by both cohesiveness and adhesion, depends on intermolecular physicochemical interactions between biopolymers, including polysaccharides as well as proteins and cations, for instance, Ca^{2+} (Flemming and Wingender 2010; Mayer et al. 1999). In contrast, other metal cations (Chen and Stewart 2002), including silver (Ag^{+}) ions, have been reported to impair the mechanical stability of a biofilm (Chaw et al. 2005). This has been attributed to their ability to bind to functional groups of proteins and polysaccharides leading to a decrease in the number of possible intermolecular interactions and impairing cohesiveness (Chaw et al. 2005). Because Ag NPs are known to release Ag^{+} ions and may even serve as a continuous source for ions (Navarro et al. 2008; Kroll et al. 2014, 2016; Gil-Allué et al. 2015; Li and Lenhart 2012; Metreveli et al. 2016), exposure to Ag NPs might lead to adverse effects on the mechanical stability of biofilms. Mechanical stability is strongly connected to sediment stabilization, namely, biostabilization in riverine systems (Gerbersdorf and Wieprecht 2015). Biostabilization results in cohesion of sediments against hydrodynamic forces, and continually increasing concentrations of Ag NPs in the aquatic environment might impair this substantial ecosystem function. Moreover, because it has been reported that Ag NPs accumulate within biofilms (Ikuma et al. 2015), and the accumulation of Ag NPs can result in enhanced local concentrations of released Ag^{+}, it is crucial to assess the consequences of this pollutant for mechanical stability.

Although there are many studies reporting adverse effects of Ag NPs on the biomass and structure of biofilms (Schaumann et al. 2015; González et al. 2015), investigating the mechanical stability of bacterial biofilms in response to Ag NP has been neglected.

In the present study, we tested the hypothesis that Ag NPs in low-dose concentrations affect the functional properties of biofilms, especially the mechanical stability. In view of the difficulty of measuring the mechanical stability of biofilms (Mayer et al. 1999) and because the application of rotational viscosimeters is often limited for in situ measurements of biofilms, we developed a new approach to address this issue. This effective but simple test allowed us to investigate the cohesiveness and adhesion of biofilms in situ, i.e., without removing the biofilm from its substratum.

Furthermore, we describe changes in the descriptive (viability and biomass) and structural (EPS protein content and biofilm architecture) biofilm parameters in response to exposure to Ag NPs. For this approach, descriptive biofilm parameters were quantified with respect to protein content as well as bacterial cell membrane integrity. In addition, structural parameters were assessed by obtaining quantitative data for biofilm thickness, density, and dry mass as well as of EPS protein content. Because sodium citrate is the most commonly used stabilizing agent for Ag NPs (Tolaymat et al. 2010), biofilms formed by the autochthonous freshwater bacterium *Aquabacterium citratiphilum* (Kalmbach et al. 1997) were incubated with citrate-stabilized Ag NPs. Due to the high negative charge induced by deprotonated carboxyl groups of citrate coating, these nanoparticles are highly stable in demineralized water with the zeta potential of approximately −60 mV (Metreveli et al. 2015; Metreveli et al. 2016; Klitzke et al. 2015). The relatively low isoelectric point of pH = 2 (Klitzke et al. 2015) shows that the citrate-stabilized Ag NPs remain negatively charged in a wide pH range. *A. citratiphilum* was chosen as the representative of the *Comamonadaceae* of the *Betaproteobacteria*, a numerically dominant group of bacteria in various freshwater habitats (Newton et al. 2011). Because smaller Ag NPs are known to cause more pronounced effects on bacteria (Morones et al. 2005; Choi and Hu 2008), which is attributed to a higher surface area to volume ratio (Tolaymat et al. 2010), biofilms were treated with two different sizes of Ag NPs, namely, 30 and 70 nm. We intended to approximate environmentally relevant concentrations of Ag NPs and applied concentrations in the range of 600–2400 μg l^{-1}. This would be still at the higher end of the concentration range estimated for natural environments and would mimic a worst case scenario, such as the resuspension by flooding events.

By analyzing descriptive, structural, and functional biofilm characteristics, as exemplified by the chosen model organism, we increased the available knowledge regarding the consequences of Ag NP contamination for major biofilm ecological services.

Materials and methods

Nanoparticles and their characterization

The citrate-stabilized Ag NPs used for this study represent two different size classes, 30 and 70 nm (designated as NP30 and NP70). The NP30 dispersion was synthesized by the citrate reduction method using the same protocol as in Metreveli et al. (2015). The NP70 dispersion was purchased from particular GmbH (Hannover, Germany) at a concentration of 107 mg l^{-1}. Both nanoparticle stock dispersions were kept at +4 °C in the dark until further use.

The mean particle diameter and particle size distribution in the Ag NP dispersions were verified using dynamic light scattering (DLS). For DLS measurements, a Delsa Nano C Particle Analyzer (Beckman Coulter, Fullerton, California, USA) was used. Particle size was measured in undiluted and diluted (1:3) nanoparticle stock dispersions. Particle size is given as the z-average hydrodynamic particle diameter (the mean value ± standard deviation determined from six replicates).

Furthermore, the formation of Ag NP aggregates in modified R2A medium (Leibniz Institute DSMZ, Braunschweig, Germany) used for cultivating *A. citratiphilum* biofilms was investigated. Aggregation analysis by DLS was performed in modified R2A medium at an Ag NP concentration of 2400 μg l^{-1} over a time period of 20 h as described in Metreveli et al. (2016) for two replicate samples. Due to the limited sensitivity of DLS, at the Ag NP concentrations of 600 and 1200 μg l^{-1}, accurate measurements were not possible.

The release of Ag^+ from Ag NPs was investigated in modified R2A medium at Ag NP concentrations of 600, 1200, and 2400 μg l^{-1}. The Ag NP dispersions were shaken at 28 °C for 20 h in an incubator (KB 400, Binder, Tuttlingen, Germany) using a laboratory shaker (rotation velocity: 20 rpm, rotation angle: 180°, INTELLI-MIXER, NeoLab, Heidelberg, Germany). After shaking, the samples were centrifuged at 396,000×*g* for 2 h using an ultracentrifuge (SORVALL WX 90 Ultra, Thermo Electron Corporation, Osterode, Germany). The ultracentrifugation method used allows the separation of Ag NPs (cutoff: 2 nm) from the supernatant, which contains Ag^+ and ultra-small (<2 nm) Ag NPs (if present). The supernatants were analyzed by an inductively coupled plasma optical emission spectrometer (ICP-OES, 720, Agilent Technologies, Santa Clara, California, USA). More detailed information about Ag^+ release experiments are given in Metreveli et al. (2016). The concentration of silver was also measured in modified R2A medium without the addition of Ag NPs. All experiments were performed in three replicates.

Cultivation of *Aquabacterium citratiphilum* biofilms

Aquabacterium citratiphilum type strain DSM 11900 was obtained from the German Collection of Microorganisms and Cell Cultures (Leibniz Institute DSMZ, Braunschweig, Germany) and cultivated in modified R2A medium. *A. citratiphilum* biofilms were cultivated on glass microscope slides at 28 °C. For that purpose, sterile Petri dishes containing one slide each and 15-ml medium were inoculated with 5 ml of bacterial overnight suspensions (grown for 18–20 h) cultivated in R2A medium to an optical density ranging from 0.1 to 0.2 (λ = 600 nm). NP30 and NP70 were applied in three different concentrations (600, 1200, 2400 μg l^{-1}) immediately prior to inoculation. To ensure a homogenous dispersal, the dishes were shaken horizontally for 5 s after the addition of Ag NPs and the bacterial suspension. The biofilms were grown and concurrently exposed for 20 h. All experiments and measurements were conducted in triplicate.

Silver content of biofilms and media

The total silver content of biofilms treated with Ag NPs as well as the surrounding medium was determined by atomic absorbance spectroscopy (AAS, Analyst 400, Perkin Elmer, Waltham, Massachusetts, USA) following a slightly modified version of the method given by Fabrega et al. (2009b). In short, after pooling biofilm samples from two glass slides, 2-ml 65 % HNO_3 was added followed by incubation at 60 °C for 7 h to digest the organic biofilm material. After the biofilm slides had been slowly and carefully removed, the surrounding medium was freeze-dried and mixed with 1 ml Milli-Q water. For digestion, 4-ml 65 % HNO_3 was added, and the sample was incubated at 60 °C for 7 h.

Biofilm stability

To measure the mechanical stability of the biofilms in situ, the biofilm slides were transferred carefully into 50-ml tubes to avoid destruction of the biofilm material. The biofilm slides were gently fixed in the tubes in a vertical position and exposed to controlled, elevated hydrodynamic forces for 30 s using a constant water jet (flow rate 14 ml min^{-1}, sterile Milli-Q-water) generated by a high precision peristaltic pump (IPC 24, Ismatec, Wertheim, Germany). A narrow compact water jet was ensured by a sterile cannula (0.8 mm inner diameter). The cannula was located right above the biofilms (at a distance of 2–3 mm) and was moved over the sample in a randomized pattern. A flow rate of 14 ml min^{-1} was employed to achieve a flow velocity of 0.4 m s^{-1} (within the cannula) which is in the range of flow velocities reported for natural riverine systems (0.1–6 m s^{-1}). After the treatment, the slides were carefully removed from the tubes, and the dry mass of the remaining biofilm material was determined. The dry mass

of biofilms grown simultaneously under identical conditions, which had not been subjected to the mechanical stress, was used as the reference to calculate %biomass loss.

Descriptive and structural biofilm parameters

Bacterial membrane integrity

The potential cytotoxic effects of Ag NPs were assessed by testing bacterial cell membrane integrity using a LIVE/DEAD® *Bac*Light™ Bacterial Viability Kit (Molecular Probes, Eugene, USA). Stained bacteria were microscopically investigated with a Carl Zeiss Axio Imager M2 microscope (Carl Zeiss AG, Oberkochen, Germany) equipped with an EC Plan-Neofluar 100×/1.30 Oil Ph3 M27 objective and standard longpass and dual emission filter sets for green fluorescence (excitation 470/40 nm and emission 525/50 nm) and red fluorescence (excitation 550/25 nm and emission 605/70 nm). For each of the triplicate samples, 18 microscopic images were captured and used for subsequent enumeration of green fluorescent (intact cell membrane, i.e., viable cells) and red fluorescent cells (damaged cell membrane, i.e., dead cells).

Cellular and EPS protein content

Biofilms were scraped off five glass slides and pooled. The cellular and EPS protein contents were determined after separating the EPS from the cells following a slightly modified protocol given by Pan et al. (2010). In brief, biofilm samples were incubated with 0.02 M KCl and 2 % EDTA solution for 1 h and subsequent centrifugation at 3500×*g* for 30 min (Mikro 220R, Hettich, Tuttlingen, Germany). To obtain soluble cellular protein, cells were enzymatically disrupted by lysozyme (100 mg ml^{-1}) and 10 % SDS (*w*/*v*) followed by sonication (Brünig 2004, Diploma Thesis, University of Bonn, Germany, unpublished). The EPS and cellular proteins were measured photometrically using the BC-Assay Protein Quantification Kit (Uptima, Montluçon, France).

Biofilm architecture

Quantitative structural biofilm parameters were determined by gravimetry according to the method described by Arvin (1991) and Staudt et al. (2004). Biofilms from three glass slides were pooled for each measurement. For this method, the slides were drained in a vertical position for 5 min, and the biofilm wet weight was determined. After this, the samples were dried at 65 °C for 24 h, and the biofilm dry weight was determined. For calculation of wet (*mWF*) and dry mass (*mDF*), the tare weight of the slides after cleaning was determined. Biofilm thickness (*LF*) was calculated from the wet mass (*mWF*), slide surface area (*AF*), and density of the wet biofilm (ρWF). It was assumed that ρWF is 1 g cm^{-3} because biofilms consist of 98–99 % of water (Christensen and Characklis 1990). Assuming a homogeneous distribution of the biofilm on the glass slide, (*LF*) was calculated using the following equation:

$$\rho F = \frac{mDF}{\frac{mWF}{\rho WF}} \quad (1)$$

The mean biofilm density (without water) (ρF) was calculated from:

$$L_F = \frac{mWF}{\rho WF \cdot A_F} \quad (2)$$

Data analysis

All the experimental data were checked for normal distribution by the Shapiro-Wilk test (Gardener 2012) using the open source software package "R" (R Core Team 2013). Differences between the control and Ag NP treatments were analyzed by one-way ANOVA followed by a Tukey's post hoc test. A correlation test to examine links between concentrations of Ag NPs (NP30) and biomass loss from the biofilms were analyzed by Spearman's rank correlation.

Ag content as well as cellular and EPS protein contents in biofilms grown and treated in parallel under identical conditions were qualitatively normalized per biofilm dry mass. Thus, we normalized μg Ag mass per mg biofilm dry mass and μg cellular or EPS protein mass per mg biofilm dry mass.

Results

Colloidal stability and dissolution of Ag NPs

The particle sizes in the NP30 and NP70 initial dispersions determined by DLS were 32 ± 3 and 97 ± 3 nm, respectively, which is given in the Electronic Supporting Material (ESM 1). While the mean particle size measured in NP30 initial dispersion was comparable to the target size of 30 nm, the NP70 initial dispersion showed higher than the nominal size (70 nm) given by the manufacturer. Most likely, particles in the NP70 dispersion were slightly aggregated. If aggregates are present in the dispersion, DLS can lead to an overestimation of the particle size because the light scattering intensity is proportional to the sixth power of the particle diameter (Finsy 1994). Furthermore, the polydispersity index determined for NP30 (0.40 ± 0.02) was higher than for NP70 (0.20 ± 0.01) indicating broader particle size distribution for NP30 than for NP70.

The time-resolved DLS measurements performed in the R2A medium during the 20-h exposure showed an increasing particle diameter (from 32 ± 3 to 61 ± 6 nm for NP30 and from 97 ± 3 to 217 ± 72 nm for NP70) (ESM 2). This increase suggests only a moderate aggregation of Ag NPs in the medium for the experimental conditions used in this study, which may be due to the partial steric stabilization of the nanoparticles by the medium component polysorbate 80, a nonionic surfactant (Li and Lenhart 2012). These results are in agreement with our other study showing much less aggregation of Ag NPs in R2A than in media used for (eco-)toxicological studies with aquatic invertebrates (Metreveli et al. 2016). In contrast to the results reported by Zhang et al. (2011), no significant effect of the initial particle size on the aggregation rate could be observed although the particle number concentration in NP30 dispersion was higher than in NP70 dispersion at the same mass concentration. In summary, the moderate aggregation status for both particle sizes suggests marginal sedimentation of the Ag NPs, which therefore allows a dose-related interpretation of our data.

The experiments for Ag NP dissolution showed a small release of Ag^+ (<2 nm) in R2A medium (Table 1). For NP30, the concentration of released Ag^+ was below the limit of quantification of ICP-OES. The release of silver could be determined only for NP70 dispersions. However, the Ag^+ concentrations for NP70 were close to the LOQ, and only 0.27 to 0.55 % of the initially spiked total silver was released into the R2A medium. The marginal dissolution of Ag NPs in R2A medium is in a good agreement with our previous study showing that the release of silver was lower in R2A medium than in other media used for (eco-)toxicological studies with aquatic invertebrates (Metreveli et al. 2016). The low level of silver released into R2A medium is most likely a result of adsorption by proteins or protein fragments in the medium.

Enrichment of Ag NPs in biofilms

Figure 1 illustrates the concentration of Ag in biofilms for both Ag NP size classes depending on the initial Ag NP concentration. Uptake of Ag NPs by biofilms comprises Ag attached to the biofilm cells, Ag in the biofilm EPS, and sedimented on top of the biofilms. The digestion method used for the sample preparation prior to the Ag measurement does not allow the differentiation between Ag^+ and Ag NPs and enables only the determination of the total Ag content in the biofilms. The precise speciation of the Ag in the biofilms should be clarified in further studies. It is apparent that the increase in Ag concentration in the biofilms was well correlated with the initial NP30 concentration (Fig. 1). The concentration of incorporated silver increased from 4600 ± 330 to 9400 ± 517 to 18,000 ± 1051 μg l^{-1}, which is a large (~8-fold) increase in the Ag concentration in the biofilms compared to the initial Ag NP concentration applied. This corresponds to an increase of Ag content in biofilm from 0.65 ± 0.05 (600 μg l^{-1} NP30) to 1.19 ± 0.07 (1200 μg l^{-1} NP30) to 2.41 ± 0.14 (2400 μg l^{-1} NP30) μg per mg biofilm dry mass. These results indicate that the absorption capacity of 20-h-old biofilms has not yet reached a maximum saturation level for this particle size. The Ag contents for NP70, ranging from 4400 ± 727 to 12,000 ± 1007 μg l^{-1}, exhibited declining enrichments of silver with increasing initial NP70 concentrations, i.e., the enrichment decreased from 7-fold to 5-fold (Fig. 1). This enrichment corresponds to 0.59 ± 0.10 (600 μg l^{-1} NP70), 1.28 ± 0.10 (1200 μg l^{-1} NP70), and 1.78 ± 0.15 (2400 μg l^{-1} NP70) μg Ag mass per mg biofilm dry mass. The Ag content for NP70 was significantly lower ($p < 0.05$) compared with that for NP30 at an initially applied concentration of 2400 μg l^{-1} Ag NP. Thus, the biofilms may have a slightly reduced capacity to concentrate silver from NP70 as the initial applied concentrations increased compared with NP30. Nevertheless, it is evident from the results that biofilms of *A. citratiphilum* exhibit a large capacity to accumulate and concentrate Ag from both Ag NP size classes. This finding was confirmed by measuring the Ag content in the medium surrounding the biofilm, where the Ag concentrations became depleted to approximately one sixth of the initial concentration (ESM 3).

Biofilm stability

The treatment with hydrodynamic forces generated by a defined water jet led to a partial detachment of the biofilm

Table 1 Concentration (μg l^{-1}) of Ag^+ (<2 nm) in R2A medium in the absence and presence of Ag NPs (mean value ± standard deviation from three replicate experiments)

	Ag NP concentration (μg l^{-1})			
	0	600	1200	2400
R2A without Ag NP	< LOD	-	-	-
R2A with NP30	-	< LOD [a]	< LOD [a]	< LOQ [b]
R2A with NP70	-	3.3 ± 2.5 (0.55)	5.8 ± 3.3 (0.48)	6.4 ± 0.4 (0.27)

[a] LOD: limit of detection (1.2 μg l^{-1})

[b] LOQ: limit of quantification (2.1 μg l^{-1})

The values in parentheses are the amounts (%) of released silver related to the initially spiked total silver

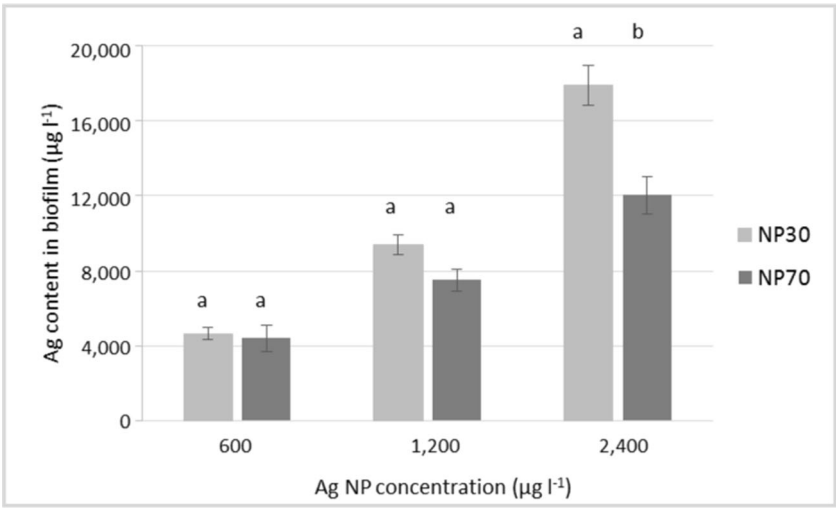

Fig. 1 The Ag contents of biofilms in the presence of initial concentrations of NP30 (*light gray*) or NP70 (*dark gray*) after 20-h incubation. The Ag contents are given as µg Ag per l biofilm volume. *Bars* represent the mean value, and *error bars* represent the standard deviation of three replicates. *Different letters* denote statistically significant differences ($p < 0.05$) between Ag contents of NP30 and NP70 for each initially applied concentration

material linked to the cohesive and adhesive strength of the biofilms. Control biofilms (0 µg l^{-1} Ag NPs) lost on average as little as 38 ± 12 % of the biomass (Fig. 2a, b). As a consequence of exposure to NP30, the mechanical biofilm stability was even more affected, with losses in the mean biomass of 44 ± 17 to 55 ± 12 to 65 ± 14 % associated with increasing concentrations of NP30 from 600 to 2400 µg l^{-1} (Fig. 2a). The biomass losses were not statistically significantly different to those of the control (0 µg l^{-1} Ag NP), but Spearman's rank correlation test revealed that this upward trend in biomass loss was positively correlated ($p < 0.05$) with increased concentrations of NP30 from 0 to 2400 µg l^{-1} (Fig. 2c). Concentrations of 600, 1200, and 2400 µg l^{-1} of NP70 produced statistically significant ($p < 0.05$) biomass losses of 57 ± 4, 60 ± 4, and 58 ± 5 %, respectively (Fig. 2b). Interestingly, the biomass loss induced by NP70 was similar for each concentration applied. In general, these data indicate that Ag NPs affect the mechanical stability, the adhesion, and cohesiveness, of the biofilms of *A. citratiphilum*.

Descriptive and structural biofilm parameters

Bacterial membrane integrity

No statistically significant ($p > 0.05$) differences in bactericidal activity was detectable after exposure to NP30 (Fig. 3a) or NP70 (Fig. 3b). The relative abundance of green biofilm cells (intact cell membrane, i.e., viable cells) remained stable at an average of 63 ± 7–12 % regardless of the Ag NP concentration and size (Fig. 3a, b).

Cellular and EPS protein content

The cellular protein contents decreased slightly after treatment with 600 to 2400 µg l^{-1} of NP30 or NP70 (Fig. 4a, b). Nevertheless, this trend was not statistically significant ($p > 0.05$). The cellular protein contents of biofilms fell from 506 ± 78 to 475 ± 44 to 420 ± 30 µg ml^{-1} in the presence of NP30 compared with the content of cells of untreated biofilms (0 µg l^{-1} Ag NP), which contained 532 ± 88 µg ml^{-1} protein (Fig. 4a). Cellular proteins were reduced from 489 ± 36 to 474 ± 17 to 466 ± 42 µg ml^{-1} with rising concentrations of NP70 (Fig. 2b). This corresponds to 64.34 ± 12.01, 64.84 ± 6.85, 56.12 ± 17.07, and 52.48 ± 3.31 µg cellular protein per mg biofilm dry mass for concentrations from 0 to 2400 µg l^{-1} NP30. In the presence of 0–2400 µg l^{-1} NP70, cellular protein content accounts for 64.34 ± 12.01, 58.08 ± 9.47, 74.10 ± 26.25, and 57.89 ± 11.19 µg per mg biofilm dry mass.

The EPS protein contents were not significantly different ($p > 0.05$) when the biofilms were exposed to NP30 at concentrations of 600–2400 µg l^{-1} or to 0 µg l^{-1} Ag NPs (untreated control biofilms) (Fig. 4c). The control biofilms and treated biofilms produced comparable EPS protein contents, which varied from 1700 ± 370 to 2500 ± 739 µg ml^{-1} in the presence of NP30 at concentrations of 600–2400 µg l^{-1} (Fig. 4c). Similar to the NP30 results, no significant ($p > 0.05$) alterations in the EPS protein contents were observed in the presence of 600–2400 µg l^{-1} NP70 compared with the control (0 µg l^{-1} Ag NPs) (Fig. 4d). The mean EPS protein content ranged between 1800 ± 123 and 2200 ± 188 µg ml^{-1} for all the treatments. The corresponding EPS protein content for control and for all treatments with NP30 or NP70 varies from 200.96 ± 12.68 and 350.91 ± 124.29 µg per mg biofilm dry mass .

In general, comparing Figs. 4a with b and 4c with d shows that the EPS protein contents clearly exceeded the cellular protein contents. Though a marginal contamination of cellular components with the EPS due to the extraction method cannot be fully excluded, taking the total biofilm protein, composed of cellular and EPS protein, into account, the EPS protein

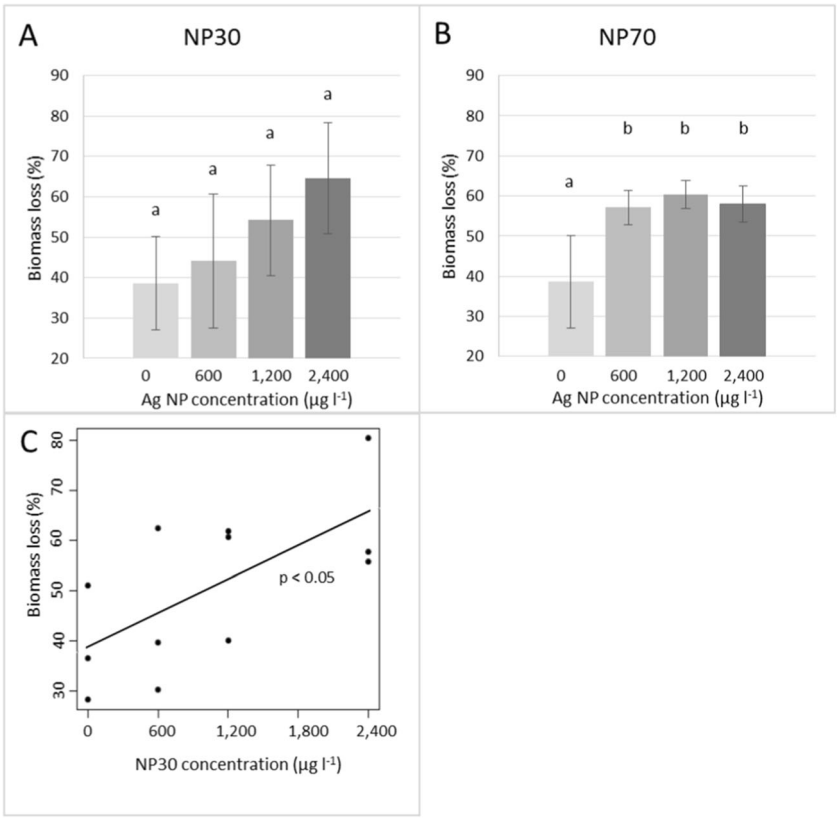

Fig. 2 Loss of biofilm biomass in the control and after 20-h incubation with NP30 (**a**) or NP70 (**b**) at initial concentrations of 600, 1200, and 2400 μg l^{-1}. *Bars* represent the mean value, and *error bars* represent the standard deviation of three replicates. *Different letters* denote statistically significant differences ($p < 0.05$). The values with the same letters are not statistically different. Scatter plot to show the significant positive correlation as calculated with Spearman's rank correlation test ($p < 0.05$) between applied concentrations of NP30 (μg l^{-1}) and biomass loss (%) (**c**). The *solid line* represents the linear fit of the mean of three replicates for each measurement

represents 79–83 % of the total protein in the biofilms. These data are in accordance with the fact that in most biofilms, the dry mass of the EPS matrix is significantly higher than the dry mass of the microorganisms and can account for up to 90 % of the total dry mass (Flemming and Wingender 2010).

Biofilm architecture

The biofilms contained between 0.04 and 0.12 mg cm^{-2} dry mass (Fig. 5a) and were 102–147 μm thick (Fig. 5b); they thus had a biofilm density ranging from 0.003 to 0.01 g cm^{-3} (Fig. 5c). It is evident from the results that the presence of NP30 or NP70 did not produce any statistically significant ($p > 0.05$) alterations in the biofilm architecture for the parameters determined in this study.

Discussion

Speciation of Ag NPs and enrichment in the biofilm

Because Ag NPs showed only slight aggregation for both particle sizes and negligible Ag^+ contents in the Ag NP suspensions and in the R2A medium, marginal sedimentation and

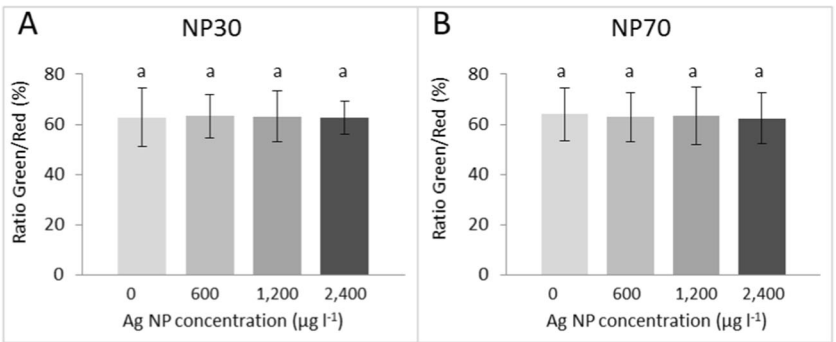

Fig. 3 *A. citratiphilum* viability as measured with the LIVE/DEAD® *Bac*Light™ Bacterial Viability Kit after exposure to Ag NPs. Viability in the control and after 20-h exposure to the three initial concentrations of NP30 (**a**) or NP70 (**b**). *Bars* represent the mean value, and *error bars* represent the standard deviation from three replicates. No statistically significant differences between treatments (0–2400 μg l^{-1}) were observed ($p > 0.05$)

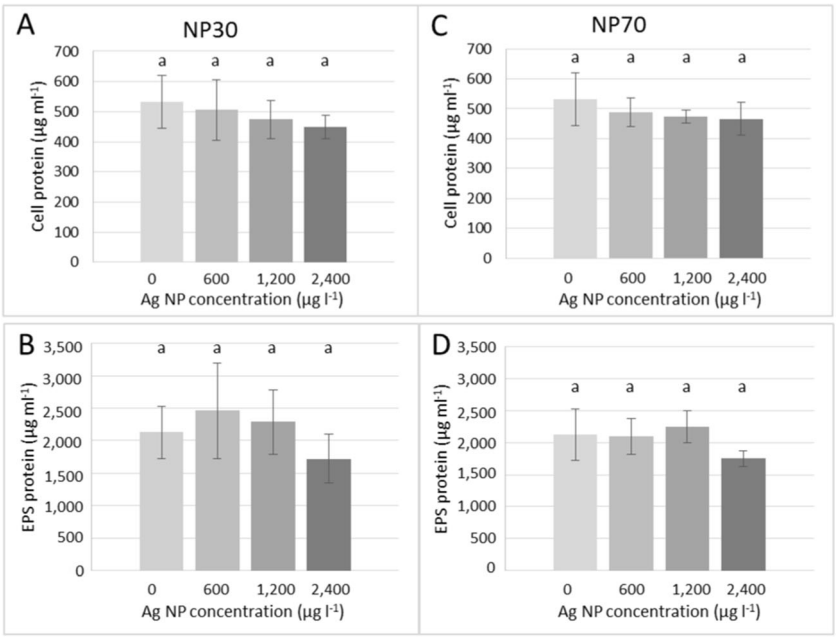

Fig. 4 Biofilm protein content (µg ml^{-1} biofilm) in the control and after 20-h exposure to the three initial concentrations of NP30 (**a**, **b**) or NP70 (**c**, **d**). *Bars* represent the mean value, and *error bars* represent the standard deviation from three replicates. No statistically significant differences between treatments (0–2400 µg l^{-1}) identified by identical letters were observed ($p > 0.05$)

negligible dissolution of the Ag NPs were assumed, which allowed the dose-related interpretation of our data.

It is widely accepted that the toxicity and antimicrobial effects of Ag NPs are caused by bioavailable Ag^+ ions released from nanoparticles by oxidative dissolution (Boenigk et al. 2014; Sotiriou and Pratsinis 2010). Consequently, the total absence of toxic and antimicrobial effects on the descriptive and structural biofilm parameters observed in this study is most probably associated with the very low Ag^+ ion release determined in our experiment. The Ag^+ ions released from the rather low doses of Ag NPs could not be detected for NP30 (<LOQ) and was very low for initially spiked NP70. Furthermore, reducing sugars within the EPS (Kang et al. 2014), Ag^+ chelating compounds, either dissolved in the

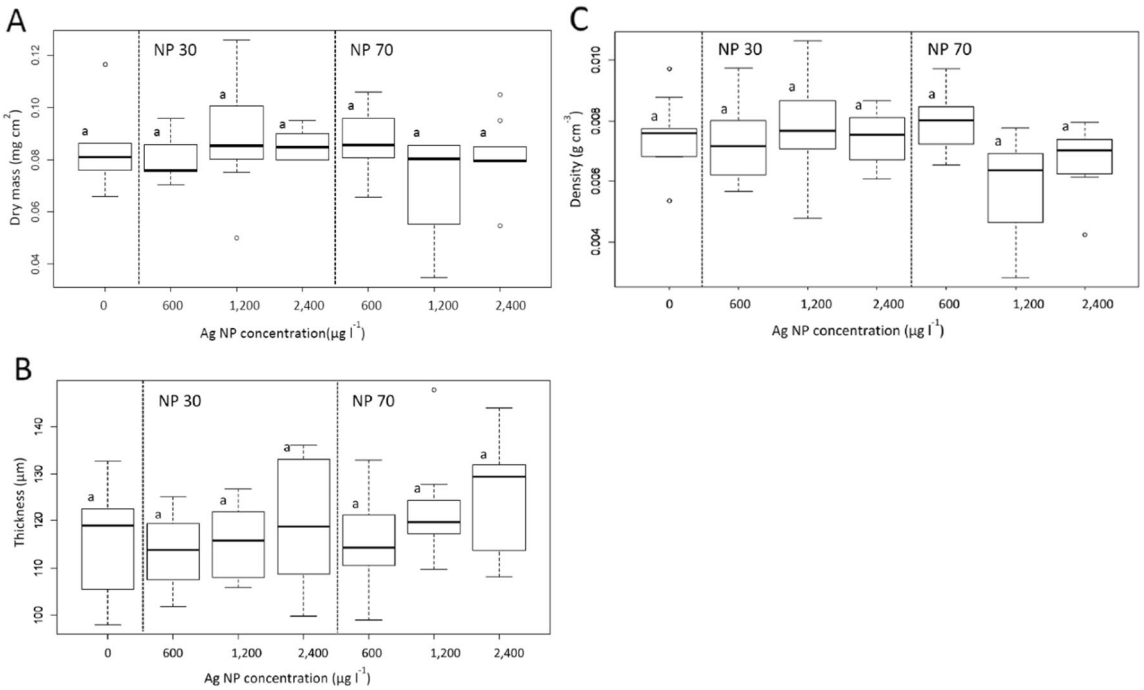

Fig. 5 Structural parameters of biofilms obtained by gravimetric measurements in the control and after 20-h exposure to the three initial concentrations of NP30 or NP70: dry mass (mg cm^{-2}) (**a**), biofilm thickness (µm) (**b**), and biofilm density (g cm^{-3}) (**c**). *Stripes* show the medians, *boxes* show the inter quartiles, the *dots* show the outliers, and the *whiskers* extend to the extremes. No statistically significant differences between treatments (0–2400 µg l^{-1}) were observed ($p > 0.05$)

aqueous phase or as functional groups of EPS (Wirth et al. 2012), and the coating of Ag NPs with sodium citrate antagonized the antibacterial activity of the Ag^+ ions and Ag NP (Pillai and Kamat 2004). In addition, the expected formation of Ag NP protein coronae due to proteins and/or protein fragments in our medium (Metreveli et al. 2016) can also influence the antibacterial activity of Ag NPs (Duran et al. 2015). Proteins sorbed onto Ag NP surfaces can form protein coronae (Kakinen et al. 2013; Chen et al. 2012) and hinder the diffusion and adsorption of oxidants onto Ag NPs (Ostermeyer et al. 2013; Kakinen et al. 2013). Hence, we assume that the chemical environment in the medium strongly influences toxicity as proposed elsewhere (Tejamaya et al. 2012; Metreveli et al. 2016). Notwithstanding the negligible toxic effect of Ag NPs, one should keep in mind that Ag NPs (i) may serve as a continual source of Ag^+ ions (Navarro et al. 2008) and (ii) produce reactive oxygen species in the oxidation process, which also have been reported to cause negative effects on microorganisms (Pillai et al. 2014).

Because the biofilms in this study revealed a high uptake capacity for Ag NPs, which indicates cumulative enrichment, continuously released Ag^+ ions as well as the production of reactive oxygen species might be relevant.

Unaffected descriptive and structural biofilm parameters

Despite the significant enrichment of Ag NPs in the biofilms, the concentrations applied in this study did not result in clear adverse effects on the viability of cells, cell protein content, architecture, and EPS protein content. This is in contrast to previous studies reporting that Ag NPs affect bacterial planktonic cells (Choi et al. 2008; Dror-Ehre et al. 2009; Hwang et al. 2008; Lok et al. 2006; Morones et al. 2005; Sondi and Salopek-Sondi 2004; Silver et al. 2006; Reinsch et al. 2012; Choi et al. 2010) as well as bacterial biofilms (Choi et al. 2010; Dror-Ehre et al. 2010; Fabrega et al. 2009b, 2011). Generally, Ag NPs are claimed to inhibit enzyme activity and essential cellular processes, including DNA transcription and bacterial respiration (Choi et al. 2008; Hwang et al. 2008; Silver et al. 2006; Dror-Ehre et al. 2010). Impacts of Ag NPs on descriptive and structural biofilm parameters have also been described (Choi et al. 2010; Dror-Ehre et al. 2010; Fabrega et al. 2009b, 2011; Sheng and Liu 2011). Because methodologies to assess Ag NP's toxicity differ among the literature, there is a certain discrepancy in results reporting effects of Ag NPs (Moreno-Garrido et al. 2015). However, in most of these studies, the concentration of Ag NPs applied to evoke these effects was ~10–80-fold higher (ranging from 38 mg l^{-1} (Choi et al. 2010) to 45 mg l^{-1} (Dror-Ehre et al. 2010) to 200 mg l^{-1} (Sheng and Liu 2011)) than in this study, in which low-dose concentrations of Ag NPs from 600 to 2400 μg l^{-1} were chosen. Although in the work of Fabrega et al. (2009b), thinning effects on biofilms of *Pseudomonas putida* treated with Ag NPs of concentrations comparable to those used in our study were observed, the levels of released dissolved Ag^+ ions were higher than in our medium. Released dissolved Ag^+ ions from Ag NPs accounted for 1–2 % depending on the pH value of the total applied Ag in the culture medium (Fabrega et al. 2009a), which is 2–7-fold higher than the released Ag^+ ions (0.27–0.55 %) in our medium. In the study of Fabrega et al. (2009b), minimal Davis medium (MDM) was used, which does not contain proteins or their fragments or surfactants. Furthermore, MDM exhibits much higher ionic strength (55 mmol l^{-1}) than the R2A medium (8.75 mmol l^{-1}) used in our work, what is in the range of ionic strength of natural river water (5–10 mmol l^{-1}) (Metreveli et al. 2015). Hence, the chemical composition of R2A medium seems to hamper the (bio)availability of Ag^+ ions. In summary, this emphasizes that not only the concentration of the applied Ag NPs but rather the concentration of bioavailable Ag^+ ions, which depends on the chemical composition of the environment, is relevant to the antimicrobial effects.

The marginal reduction in cellular protein content suggests that the bacterial cells might have been slightly reduced in their total abundance or their sizes. Thus, subtle adverse effects on the biofilms cells caused by Ag NPs, which includes released Ag^+ ions and/or reactive oxygen species produced in the oxidation process, cannot be entirely excluded. This observation might be associated with a slow growth rate, which has been interpreted as a resistance mechanism occurring under antibiotic stress in bacterial biofilms (Mah and O'Toole 2001). A similar relationship has been reported for reduced colony sizes after exposure to metal nanoparticles (Baek and An 2011). Furthermore, EPS is capable to bind heavy metal cations (such as Cu^{2+}, Pb^{2+}, and Zn^{2+}) because of the abundance of chelating groups (e.g., amino, carboxyl, and phenol) (Teitzel and Parsek 2003). Thus, EPS may act as a permeability barrier hindering also the diffusion and adsorption of Ag NPs and Ag^+ ions onto the cells, which are embedded in the EPS matrix (Kang et al. 2014). Hence, the toxicity of Ag NPs and Ag^+ ions might have been attenuated by EPS. In summary, these results show that at the concentration range investigated in this study, a subtle stress-induced response to exposure to Ag NPs cannot be excluded but is expected in a relatively limited range.

Ag NPs affect the stability of biofilms

Although the low silver concentrations exhibited no antimicrobial activity, sublethal effects on the mechanical stability of the biofilms were observed. Generally, cohesiveness within the biofilm and adhesion of the biofilm to surfaces are mediated by complex physicochemical interactions, including ionic attractive forces, hydrogen bonds, van der Waals interactions, and repulsive and/or attractive forces between macromolecules, including proteins and polysaccharides and ions

(Chaw et al. 2005; Flemming and Wingender 2010). Consequently, it has been reported that Ag^+ ions, because of their high reactivity, bind to biological molecules, including proteins and polysaccharides within the EPS (Chaw et al. 2005). Thus, Ag NPs or released free Ag^+ ions may be involved in physicochemical interactions between the different functional groups of the EPS, altering cohesive forces within the biofilm matrix. As observed in silver release experiments, in contrast to NP30, the dispersion of NP70 showed a low but measurable release of Ag^+ ions. This is in a good agreement with the greater effects on the mechanical stability in the case of NP70 compared with NP30.

Furthermore, fimbria and/or flagella of the biofilm bacteria ensure attachment to a surface on the bottom of the biofilms (Gerbersdorf and Wieprecht 2015). The slightly reduced cell protein content associated with increased concentrations of NP30 and NP70, interpreted as a reduced abundance of biofilm cells and/or smaller cells, might be accompanied by a decrease in the total amount of fimbria and flagella. Consequently, this might also have contributed to the decreased adhesion observed.

In addition, the medium ingredient polysorbate 80, which serves as both carbon and energy source for *A. citratiphilum*, is known for its interaction with macromolecules including proteins (Wang et al. 2008). Because polysorbate 80 might have been interacting with proteins in the EPS, its contribution to the observed weakened biofilm stability cannot be fully excluded.

Nevertheless, our results provide a compelling evidence for a negative impact of Ag NPs on the mechanical stability of biofilms. This might raise concern for a possible impairment of biostabilization in riverine systems (Gerbersdorf and Wieprecht 2015), because the mechanical stability of biofilms is strongly connected to sediment stabilization. Future work focusing on biostabilization impairment by Ag NPs should be addressed through methods such as MagPI (Larson et al. 2009) that targets precisely at biostabilization.

Putative particle size-dependent effects

In contrast to other studies (Radniecki et al. 2011; Pal et al. 2007; Sadeghi et al. 2012), our results did not confirm that smaller Ag NPs trigger greater effects than larger Ag NPs at the low Ag NP concentrations applied in this study. It has been suggested that smaller sized particles, due to their higher surface area to volume ratio (Tolaymat et al. 2010), show higher toxicity potential than larger particles (Morones et al. 2005; Tolaymat et al. 2010; Choi and Hu 2008). Because the initial size of NP30 almost doubled by increasing from 32 to 61 nm during exposure time of 20 h, the surface area to volume ratio might become less relevant, what might be accompanied by a decrease in toxicity potential.

Regarding the enrichment of Ag NPs in biofilms, a (partially significant) higher uptake capacity was observed for NP30 compared with NP70. The uptake of Ag by biofilms suggested an attachment of Ag NPs to biofilm cells and biofilm EPS. Consequently, this difference is most likely explainable by the lower particle number concentration for NP70 compared to NP30 and thus a lower collision probability with bacterial cells and EPS constituents for NP70.

Furthermore, the mechanical stability of the biofilms decreased with increased concentrations of NP30, whereas the NP70 effect on the mechanical stability was relatively independent of the initial concentration used. Because our silver release experiments indicated that medium composition strongly influenced the release of Ag^+ ions (Metreveli et al. 2016), it is most likely that the chemical composition of R2A medium partly inhibits the activity of the Ag NPs as well as their size-dependent effects. Hence, to what extent the chemical effects, i.e., the availability of Ag^+ ions, and to what extent the physical effects, i.e., the nanoparticle size and shape, are more relevant to the impact of Ag NPs on the mechanical stability of biofilms, needs to be clarified in further studies.

Conclusions

The experimental approach used in this study allowed us to characterize the descriptive, structural, and functional characteristics of *A. citratiphilum* biofilms exposed to Ag NPs. Our experimental results indicate that Ag NPs of 30 and 70 nm did not have significant impacts on the descriptive and structural parameters of the biofilms after 20-h exposure within the concentration range of 600–2400 μg l^{-1}. Nevertheless, we observed a cumulative enrichment of Ag NPs in biofilms. Because *A. citratiphilum* as a representative member of a widespread bacterial freshwater clade was chosen to be confronted with concentrations of Ag NPs close to environmentally relevant conditions, our approach may reflect nearly normal responses of natural freshwater biofilms to Ag NPs. The cumulative enrichment of Ag NPs in biofilms may be a general response and therefore expected for more complex, native multispecies biofilms, which might lead to "poisoned" nutrients for grazers inside the food web. This enrichment clearly underlines the importance of biofilms and organic matter in general for the retention of metals (or nanoparticles) in the environment (Harrison et al. 2007). In this context, it is an important issue that future studies define the speciation of the Ag in the biofilms and distinguish between the effects on biofilms mediated by Ag NPs and those mediated by Ag^+ ions.

In the first study, to investigate the impact of Ag NPs on the mechanical stability of bacterial biofilms, we successfully demonstrated a qualitative approach to assess the consequences of hydrodynamic forces on biofilms in their natural

condition. Thus, conclusions might be drawn about the negative impact of Ag NPs on the mechanical stability of natural biofilms in the aquatic environment. Aquatic biofilms are affected by strong currents in rivers and tidal systems and must resist strong shear forces and detachment. The cohesiveness of sediments depends on EPS production and biofilm formation. Consequently, the observed Ag NP-mediated decrease in biofilm stability might indicate that not only the ability of biofilms to withstand potentially harsh hydrodynamic conditions in flowing waters is diminished, but also detrimental effects on sediments in river beds may occur.

In order to support this assumption, further work applying rheological measurements to unravel the impact of Ag NPs on cohesiveness and viscoelastic biofilm properties and applying MagPI to address biostabilization in response to Ag NP exposure is in progress.

Acknowledgments This study was supported by the German Research Foundation (DFG; Research unit INTERNANO: FOR 1536, subprojects BIOFILM MA3273/3-1 and MASK SCHA849/16). We thank U. Bange for the AAS measurements and K. Hoffmann, J. Tepper, C. Sodemann, and B. Schmidt for technical assistance. We are also grateful to Dr. W. Fey for the ICP-OES measurements.

Compliance with ethical standards

Notes The authors declare no competing financial interest.

References

Arvin E (1991) Biodegradation kinetics of chlorinated aliphatic hydrocarbons with methane oxidizing bacteria in an aerobic fixed biofilm reactor. Water Res 25:873–881

Baek YW, An YJ (2011) Microbial toxicity of metal oxide nanoparticles (CuO, NiO, ZnO, and Sb2O3) to *Escherichia coli*, *Bacillus subtilis*, and *Streptococcus aureus*. Sci Total Environ 409:1603–1608

Blaser SA, Scheringer M, MacLeod M, Hungerbühler K (2008) Estimation of cumulative aquatic exposure and risk due to silver: contribution of nano-functionalized plastics and textiles. Sci Total Environ 390:396–409

Boenigk J, Beisser D, Zimmermann S, Bock C, Jakobi J, Grabner D et al (2014) Effects of silver nitrate and silver nanoparticles on a planktonic community: general trends after short-term exposure. PLoS One 9(4)

Chaw KC, Manimaran M, Tay FE (2005) Role of silver ions in destabilization of intermolecular adhesion forces measured by atomic force microscopy in *Staphylococcus epidermidis* biofilms. Antimicrob Agents Chemother 49:4853–4859

Chen X, Stewart PS (2002) Role of electrostatic interactions in cohesion of bacterial biofilms. Appl Microbiol Biotechnol 59:718–720

Chen R, Choudhary P, Schurr RN, Bhattacharya P, Brown JM, Ke PC (2012) Interaction of lipid vesicle with silver nanoparticle-serum albumin protein corona. Appl Phys Lett 100:013703

Choi O, Hu Z (2008) Size dependent and reactive oxygen species related nanosilver toxicity to nitrifying bacteria. Environ Sci Technol 42: 4583–4588

Choi O, Deng KK, Kim NJ, Ross L, Surampalli RY, Hu Z (2008) The inhibitory effects of silver nanoparticles, silver ions, and silver chloride colloids on microbial growth. Water Res 42:3066–3074

Choi O, CP Y, Fernández GE, Hu Z (2010) Interactions of nanosilver with *Escherichia coli* cells in planktonic and biofilm cultures. Water Res 44:6095–6103

Christensen BE, Characklis WG (1990) Physical and chemical properties of biofilms. Methods Enzymol 93

Dror-Ehre A, Mamane H, Belenkova T, Markovich G, Adin A (2009) Silver nanoparticle–*E. coli* colloidal interaction in water and effect on *E. coli* survival. J Colloid Interface Sci 339:521–526

Dror-Ehre A, Adin A, Markovich G, Mamane H (2010) Control of biofilm formation in water using molecularly capped silver nanoparticles. Water Res 44:2601–2609

Duran N, Silveira CP, Duran M, Martinez DST (2015) Silver nanoparticle protein corona and toxicity: a mini-review. J Nanobiotechnol 13

Fabrega J, Fawcett SR, Renshaw JC, Lead JR (2009a) Silver nanoparticle impact on bacterial growth: effect of pH, concentration, and organic matter. Environ Sci Technol 43:7285–7290

Fabrega J, Renshaw JC, Lead JR (2009b) Interactions of silver nanoparticles with *Pseudomonas putida* biofilms. Environ Sci Technol 43:9004–9009

Fabrega J, Zhang R, Renshaw JC, Liu WT, Lead JR (2011) Impact of silver nanoparticles on natural marine biofilm bacteria. Chemosphere 85:961–966

Finsy R (1994) Particle sizing by quasi-elastic light scattering. Adv Colloid Interf 52:79–143

Flemming HC, Wingender J (2010) The biofilm matrix. Nat Rev Microbiol 8:623–633

Gardener M (2012) Exploring data – looking at numbers. In: statistics for ecologists using R and excel. Pelagic Publishing, Exeter, p. 76

Gerbersdorf SU, Wieprecht S (2015) Biostabilization of cohesive sediments: revisiting the role of abiotic conditions, physiology and diversity of microbes, polymeric secretion, and biofilm architecture. Geobiology 13:68–97

Gil-Allué C, Schirmer K, Tlili A, Gessner MO, Behra R (2015) Silver nanoparticle effects on stream periphyton during short-term exposures. Environ Sci Technol 49:1165–1172

González AG, Mombo S, Leflaive J, Lamy A, Pokrovsky OS, Rols JL (2015) Silver nanoparticles impact phototrophic biofilm communities to a considerably higher degree than ionic silver. Environ Sci Pollut Ress 22:8412–8424

Gottschalk F, Sun T, Nowack B (2013) Environmental concentrations of engineered nanomaterials: review of modeling and analytical studies. Environ Pollut 181:287–300

Harrison JJ, Ceri H, Turner RJ (2007) Multimetal resistance and tolerance in microbial biofilms. Nat Rev Microbiol 5:928–938

Hwang ET, Lee JH, Chae YJ, Kim YS, Kim BC, Sang BI, MB G (2008) Analysis of the toxic mode of action of silver nanoparticles using stress-specific bioluminescent bacteria. Small 4:746–750

Ikuma K, Decho AW, Lau BL (2015) When nanoparticles meet biofilms—interactions guiding the environmental fate and accumulation of nanoparticles. Front Microbiol 6:591

Kaegi R, Voegelin A, Ort C, Sinnet B, Thalmann B, Krismer J et al (2013) Fate and transformation of silver nanoparticles in urban wastewater systems. Water Res 47:3866–3877

Kakinen A, Ding F, Chen PY, Mortimer M, Kahru A, Ke PC (2013) Interaction of firefly luciferase and silver nanoparticles and its impact on enzyme activity. Nanotechnology 24:345101

Kalmbach S, Manz W, Szewzyk U (1997) Isolation of new bacterial species from drinking water biofilms and proof of their in situ dominance with highly specific 16S rRNA probes. Appl Environ Microbiol 63:4164–4170

Kang F, Alvarez PJ, Zhu D (2014) Microbial extracellular polymeric substances reduce Ag^+ to silver nanoparticles and antagonize bactericidal activity. Environ Sci Technol 48:316–322

Klitzke S, Metreveli G, Peters A, Schaumann GE, Lang F (2015) The fate of silver nanoparticles in soil solution – sorption of solutes and aggregation. Sci Total Environ 535:54–60 Special Issue: Engineered nanoparticles in soils and waters

Kroll A, Behra R, Kaegi R, Sigg L (2014) Extracellular polymeric substances (EPS) of freshwater biofilms stabilize and modify CeO2 and Ag nanoparticles. PLoS One 9(10)

Kroll A, Matzke M, Rybicki M, Obert-Rauser P, Burkart C, Jurkschat K et al (2015) Mixed messages from benthic microbial communities exposed to nanoparticulate and ionic silver: 3D structure picks up nano-specific effects, while EPS and traditional endpoints indicate a concentration-dependent impact of silver ions. Environ Sci Pollut R 1–17

Larson F, Lubarsky H, Gerbersdorf SU, Paterson DM (2009) Surface adhesion measurements in aquatic biofilms using magnetic particle induction: MagPI. Limnol Oceanogr Methods 7:490–497

Lemire JA, Harrison JJ, Turner RJ (2013) Antimicrobial activity of metals: mechanisms, molecular targets and applications. Nat Rev Microbiol 11:371–384

Li X, Lenhart JJ (2012) Aggregation and dissolution of silver nanoparticles in natural surface water. Environ Sci Technol 46:5378–5386

Lok CN, Ho CM, Chen R, He QY, WY Y, Sun H et al (2006) Proteomic analysis of the mode of antibacterial action of silver nanoparticles. J Proteome Res 5:916–924

Mah TFC, O'Toole GA (2001) Mechanisms of biofilm resistance to antimicrobial agents. Trends Microbiol 9:34–39

Mayer C, Moritz R, Kirschner C, Borchard W, Maibaum R, Wingender J, Flemming HC (1999) The role of intermolecular interactions: studies on model systems for bacterial biofilms. Int J Biol Macromol 26:3–16

Metreveli G, Philippe A, Schaumann GE (2015) Disaggregation of silver nanoparticle homoaggregates in a river water matrix. Sci Total Environ 535:35–44

Metreveli G, Frombold B, Seitz F, Grün A, Philippe A, Rosenfeldt RR et al (2016) Impact of chemical composition of ecotoxicological test media on the stability and aggregation status of silver nanoparticles. Environ Sci. Nano 3:418–433

Moreno-Garrido I, Pérez S, Blasco J (2015) Toxicity of silver and gold nanoparticles on marine microalgae. Mar Environ Res 111:60–73

Morones JR, Elechiguerra JL, Camacho A, Holt K, Kouri JB, Ramírez JT, Yacaman MJ (2005) The bactericidal effect of silver nanoparticles. Nanotechnology 16:2346

Navarro E, Piccapietra F, Wagner B, Marconi F, Kaegi R, Odzak N et al (2008) Toxicity of silver nanoparticles to *Chlamydomonas reinhardtii*. Environ Sci Technol 42:8959–8964

Newton RJ, Jones SE, Eiler A, McMahon KD, Bertilsson S (2011) A guide to the natural history of freshwater lake bacteria. Microbiol Mol Biol Rev 75(1):14–49

Ostermeyer AK, Mumuper CK, Semprini L, Radniecki T (2013) Influence of bovine serum albumin and alginate on silver nanoparticle dissolution and toxicity to *Nitrosomonas europaea*. Environ Sci Technol 47:14403–14410

Pal S, Tak YK, Song JM (2007) Does the antibacterial activity of silver nanoparticles depend on the shape of the nanoparticle? A study of the gram-negative bacterium *Escherichia coli*. Appl Environ Microbiol 73:1712–1720

Pan X, Liu J, Zhang D, Chen X, Li L, Song W, Yang J (2010) A comparison of five extraction methods for extracellular polymeric substances (EPS) from biofilm by using three-dimensional excitation-emission matrix (3DEEM) fluorescence spectroscopy. Water SA 36: 111–116

Pillai ZS, Kamat PV (2004) What factors control the size and shape of silver nanoparticles in the citrate ion reduction method? J Phys Chem B 108:945–951

Pillai S, Behra R, Nestler H, Suter MJF, Sigg L, Schirmer K (2014) Linking toxicity and adaptive responses across the transcriptome, proteome, and phenotype of *Chlamydomonas reinhardtii* exposed to silver. Proc Natl Acad Sci 111:3490–3495

R Core Team (2013) R: A language and environment for statistical computing. Version 3.0.1. R Foundation for Statistical Computing, Vienna, Austria [Online] http://www.R-project.org. Accessed Aug 08, 2013

Radniecki TS, Stankus DP, Neigh A, Nason JA, Semprini L (2011) Influence of liberated silver from silver nanoparticles on nitrification inhibition of *Nitrosomonas europaea*. Chemosphere 85:43–49

Reidy B, Haase A, Luch A, Dawson KA, Lynch I (2013) Mechanisms of silver nanoparticle release, transformation and toxicity: a critical review of current knowledge and recommendations for future studies and applications. Materials 6:2295–2350

Reinsch BC, Levard C, Li Z, Ma R, Wise A, Gregory KB et al (2012) Sulfidation of silver nanoparticles decreases *Escherichia coli* growth inhibition. Environ Sci Technol 46:6992–7000

Sadeghi B, Garmaroudi FS, Hashemi M, Nezhad HR, Nasrollahi A, Ardalan S, Ardalan S (2012) Comparison of the anti-bacterial activity on the nanosilver shapes: nanoparticles, nanorods and nanoplates. Adv Powder Technol 23:22–26

Schaumann GE, Philippe A, Bundschuh M, Metreveli G, Klitzke S, Rakcheev D et al (2015) Understanding the fate and biological effects of Ag-and TiO 2-nanoparticles in the environment: the quest for advanced analytics and interdisciplinary concepts. Sci Total Environ 535:3–19

Sheng Z, Liu Y (2011) Effects of silver nanoparticles on wastewater biofilms. Water Res 45(18):6039–6050

Silver S, Phung LT, Silver G (2006) Silver as biocides in burn and wound dressings and bacterial resistance to silver compounds. J Ind Microbiol Biot 33:627–634

Sondi I, Salopek-Sondi B (2004) Silver nanoparticles as antimicrobial agent: a case study on *E. coli* as a model for gram-negative bacteria. J Colloid Interface Sci 275:177–182

Sotiriou GA, Pratsinis SE (2010) Antibacterial activity of nanosilver ions and particles. Environ Sci Technol 44:5649–5654

Staudt C, Horn H, Hempel DC, Neu TR (2004) Volumetric measurements of bacterial cells and extracellular polymeric substance glycoconjugates in biofilms. Biotechnol Bioeng 88:585–592

Teitzel GM, Parsek MR (2003) Heavy metal resistance of biofilm and planktonic *Pseudomonas aeruginosa*. Appl Environ Microbiol 69:2313–2320

Tejamaya M, Römer I, Merrifield RC, Lead JR (2012) Stability of citrate, PVP, and PEG coated silver nanoparticles in ecotoxicology media. Environ Sci Technol 46:7011–7017

Tolaymat TM, El Badawy AM, Genaidy A, Scheckel KG, Luxton TP, Suidan M (2010) An evidence-based environmental perspective of manufactured silver nanoparticle in syntheses and applications: a systematic review and critical appraisal of peer-reviewed scientific papers. Sci Total Environ 408:999–1006

Wang W, Wang YJ, Wang DQ (2008) Dual effects of tween 80 on protein stability. Int J Pharm 347:31–38

Wirth SM, Lowry GV, Tilton RD (2012) Natural organic matter alters biofilm tolerance to silver nanoparticles and dissolved silver. Environ Sci Technol 46:12687–12696

Wölz J, Cofalla C, Hudjetz S, Roger S, Brinkmann M, Schmidt B et al (2009) In search for the ecological and toxicological relevance of sediment re-mobilisation and transport during flood events. J Soils Sediments 9:1–5

Zhang W, Yao Y, Li KG, Huang Y, Chen YS (2011) Influence of dissolved oxygen on aggregation kinetics of citrate-coated silver nanoparticles. Environ Pollut 159:3757–3762